Analyst

PAPER

View Article Online
View Journal

Cite this: DOI: 10.1039/d1an01802g

Optimizing locked nucleic acid modification in double-stranded biosensors for live single cell analysis†

Samuel A. Vilchez Mercedes, ‡[a] Ian Eder,‡[a] Mona Ahmed,[a] Ninghao Zhu[a] and Pak Kin Wong *[a,b]

Received 5th October 2021,
Accepted 20th January 2022

DOI: 10.1039/d1an01802g

rsc.li/analyst

Double-stranded (ds) biosensors are homogeneous oligonucleotide probes for detection of nucleic acid sequences in biochemical assays and live cell imaging. Locked nucleic acid (LNA) modification can be incorporated in the biosensors to enhance the binding affinity, specificity, and resistance to nuclease degradation. However, LNA monomers in the quencher sequence can also prevent the target-fluorophore probe binding, which reduces the signal of the dsLNA biosensor. This study investigates the influence of LNA modification on dsLNA biosensors by altering the position and amount of LNA monomers present in the quencher sequence. We characterize the fluorophore–quencher interaction, target detection, and specificity of the biosensor in free solution and evaluate the performance of the dsLNA biosensor in 2D monolayers and 3D spheroids. The data indicate that a large amount of LNA monomers in the quencher sequence can enhance the specificity of the biosensor, but prevents effective target binding. Together, our results provide guidelines for improving the performance of dsLNA biosensors in nucleic acid detection and gene expression analysis in live cells.

Introduction

Gene expression analyses are essential for biomedical and laboratory automation applications. However, conventional nucleic acid analysis methods typically involve cumbersome procedures, require a large number of cells, and provide qualitative or semi-quantitative results.[1] Furthermore, single cell methods are required for studying cell heterogeneity and multicellular organization of complex biological processes, such as tissue morphogenesis and tumor invasion.[2–4] Imaging techniques, such as fluorescence *in situ* hybridization (FISH), open a door into studying RNA expression in fixed cells down to the single transcript level.[5,6] Nonetheless, FISH is laborious, applicable only to fixed cells, and difficult to implement in 3D cultures. Single cell gene expression analysis methods that are sensitive, specific, and easy-to-use in both 2D and 3D culture models remain highly sought after.

Efforts have been dedicated to developing intracellular molecular probes for gene expression measurements in live cells.[7] For example, molecular beacons, DNA transformers, gold nanorods, and graphene oxide allow rapid detection of RNA in live cells.[8–11] These homogeneous biosensors often involve a fluorophore-labelled oligonucleotide probe that is complementary to the target RNA. Without a target, the fluorophore probe is quenched by an organic or nanoengineered (*e.g.*, gold nanorod and graphene) quencher. In the presence of a target, the conformational change or displacement reaction separates the quencher from the fluorophore and allows the probe to fluoresce. Among homogeneous biosensor designs, the double-stranded probe has been broadly applied for various biomedical applications.[12–17] In the double-stranded probe scheme, the fluorophore probe is hybridized with a shorter, complementary oligonucleotide sequence (quencher sequence) labelled with a quencher (Fig. 1A). The double-stranded probes provide several advantages over other designs in terms of dynamic range, signal-to-noise ratio, and hybridization kinetics.[18,19] In particular, the double-stranded probe design avoids probe self-hybridization[20] and nanoparticle aggregation,[21] and, importantly, allows additional freedom in tuning the binding affinity and competitive binding reaction by adjusting the length and concentration of the quencher sequence.[18,19]

Oligonucleotide modifications, such as locked nucleic acid (LNA), are often introduced in FISH and intracellular probes to improve the binding affinity, specificity, and resistance to nuclease degradation.[22–24] The enhanced specificity and stabi-

[a]*Department of Biomedical Engineering, The Pennsylvania State University, University Park, PA, 16802, USA. E-mail: pak@engr.psu.edu; Tel: +1-814-863-5267*
[b]*Department of Mechanical Engineering and Department of Surgery, The Pennsylvania State University, University Park, PA, 16802, USA*

†Electronic supplementary information (ESI) available. See DOI: 10.1039/d1an01802g

‡These authors contributed equally to this work.

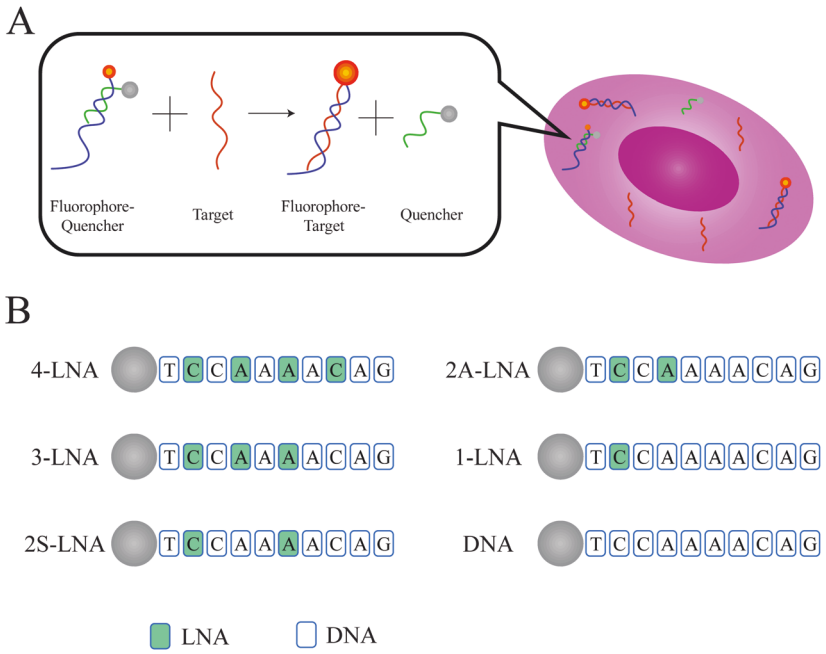

Fig. 1 A double-stranded locked nucleic acid (dsLNA) biosensor for live cell gene measurement. (A) Illustration of the working principle of the dsLNA biosensor. The biosensor consists of an oligonucleotide probe with alternating LNA monomers and a fluorophore (fluorophore probe), which hybridizes with another probe conjugated with a quencher at the 3′ end (quencher sequence). The dsLNA biosensor is transfected into live cells. With the presence of a target RNA, the quencher sequence is displaced by the target, allowing the fluorophore probe to fluoresce. (B) Illustration of quencher designs with varying amounts and positions of LNA monomers in this study. Solid green boxes represent LNA monomers while open boxes represent DNA monomers. Sequences are in the 3′ to 5′ direction.

lity are particularly important for live single cell biosensing. For example, alternating LNA–DNA monomers have shown to improve the intracellular stability of molecular beacons and double-stranded locked nucleic acid (dsLNA) probes.[15,25] Nonetheless, the influence of LNA modification in the quencher sequence has not been systematically evaluated. If the affinity between the fluorophore and quencher sequence is too high, the strong binding may prevent the displacement reaction of the target, which reduces the overall signal of the biosensor. In this study, we explored various quencher configurations to obtain an improved understanding of the dsLNA design for gene expression measurements. We designed six different quencher sequences with varying amounts and positions of LNA monomers (Fig. 1B and ESI Table 1†). We systematically characterized their affinities, sensing performance, and specificities in free solution (such as in real-time polymerase chain reaction and mix-and-measure assays).[26] We also evaluated their performance in live and fixed cells in 2D monolayers and in a 3D tumor spheroid invasion assay. The results are summarized to provide guidelines on the design of dsLNA probes for biochemical analyses.

Materials and methods

Cell culture and reagents

The human cervical cancer cell line, HeLa, was purchased from Abcam (Cambridge, MA). All cells were cultured in Dulbecco's Modified Eagle Medium containing 10% FBS and 0.1% Gentamicin (Fisher Scientific, Hampton, NH). Monolayer cell culture experiments were performed in polystyrene 24-well plates (cat. # 07-200-740, Fisher Scientific, Hampton, NH). Cells were maintained at 37 °C in 5% CO_2, and the culture medium was refreshed every 2 days. All experiments were done between passages 5–20.

Probes and synthetic targets were synthesized by Integrated DNA Technologies (San Diego, CA). All sequences were verified through the NCBI Basic Local Alignment Search Tool for nucleotides (BLASTn). Each quencher has a unique scheme of LNA and DNA monomers, ranging from a maximum of 40% LNA content to a minimum of 0% LNA content. The sequences are available in ESI Table 1.† Lipofectamine RNAiMAX (cat. #13778100, Fisher Scientific, Hampton, NH) and Block-iT™ (cat. #13750062, Fisher Scientific, Hampton, NH) were used for transfection experiments in live cells. Prior to transfection, all sequences were dissolved in 10 mM Tris–EDTA and 0.2 M NaCl before being mixed at a 3 : 1 quencher-to-probe (Q : P) ratio. The biosensors were then heated to 95 °C for 5 minutes in a dry block heater before cooling to room temperature for 10 minutes. The biosensors and the transfection reagent were diluted in Opti-MEM Medium (cat. # 31985070, Fisher Scientific, Hampton, NH) according to the manufacturer's protocol. The solution was then added to a 24 well plate seeded with cells at 90–95% confluency, according to the manufacturer's protocol.

Fluorescence plate reader assays

Free solution experiments were carried out in Flat-Bottom Corning 384-Well Microplates (cat. # 07-200-852, Thermofisher, Waltham, MA) using a Molecular Devices FlexStation 3 fluorescence plate reader. Prior to measurement, the biosensors were dissolved in 10 mM Tris–EDTA and 0.25 M NaCl and heated to 95 °C for 5 minutes. Then, the solution was allowed to cool down to room temperature for at least 10 minutes. In all our experiments, wells with 250 nM probe sequence were measured and used as the positive control (PC). Wells with buffer solution only were also measured and used as negative control (NC). Normalized fluorescence intensity of each sample was calculated with the following formula:

$$\text{Normalized intensity} = \frac{(\text{Sample signal} - \text{NC})}{(\text{PC} - \text{NC})}$$

We found this approach provides reliable results across multiple days and among different users. When the intensity value was close to the detection limit of the instrument, the normalized intensity resulted in small negative numbers (*e.g.*, −0.0003) in some cases. These values were rounded as zero.

For the quenching efficiency experiments, the wells contained 250 nM probe sequence, 0.25 M NaCl, and a variable concentration of quencher sequence in 40 μL of TE Buffer. The concentration of quencher ranged between 125 nM and 1.25 μM, corresponding with Q : P ratios of 0.5 : 1, 1 : 1, 2 : 1, 2.5 : 1, 3 : 1, and 5 : 1.

For the sensor calibration (*i.e.*, target detection) experiments, the synthetic targets were added to the biosensors after they had cooled to room temperature, then allowed to incubate at room temperature for at least 10 minutes. The wells contained 250 nM probe oligo, 750 nM quencher oligo, 0.25 M NaCl, and a variable concentration of synthetic target in 40 μL of TE Buffer. The concentration of synthetic target ranged between 25 nM and 125 μM, corresponding with target concentrations of 0.1×, 1×, 10×, 50×, 100×, and 500× the biosensor concentration. The synthetic target detection experiment was also performed with a random sequence and a β-actin mismatch target to test the specificity of the biosensors.

The signal-to-noise ratio (SNR) was then calculated using the results of the quenching efficiency and target response experiments. The background noise was considered to be the fluorescence intensity of the biosensor with a 3 : 1 Q : P ratio (referred to in the formula as 3 : 1 Background signal), in addition to the fluorescence intensity of the Tris–EDTA. The signal was the fluorescence intensity of the biosensor with the target after the background noise was subtracted. The formula for SNR is as follows:

$$\text{SNR} = \frac{(\text{sample intensity} - \text{NC})}{(3\ :\ 1\,\text{background signal} + \text{NC})}$$

RNA *in situ* hybridization

The dsLNA probes targeting β-actin and a random sequence were applied in fixed cells following the manufacturer's (Biosearch Technologies, Inc., Petaluma, CA) RNA *in situ* hybridization protocol. Briefly, HeLa cells were fixed using 3.7% (v/v) formaldehyde for 10 minutes, followed by permeabilization with 70% (v/v) ethanol for 24 hours. After rinsing with wash buffer A, the dsLNA probes were diluted in the hybridization buffer and incubated in HeLa cells for 4 hours before imaging.

3D spheroid culture

The 3D spheroid experiments were performed with Cultrex© 3D Spheroid Cell Invasion Assay Kits (cat. # 3500-096-K, Trevigen, MD) according to manufacturer's protocol. Briefly, HeLa cells were incubated with 5 μg mL^{-1} CellTracker Green CMFDA Dye (cat. # C2925, Fisher Scientific, Hampton, NH) at 37 °C for 25 minutes in a 35 mm dish for fluorescence staining. The biosensors were then transfected as previously described. Then, approximately 5000 cells per well were incubated in Spheroid Formation Extracellular Matrix in a round bottom 96 well plate and allowed to aggregate for 3 days in order to form spheroids. Then, the Invasion Matrix, a blend of collagen I and basement membrane extract, and cell culture media was added. The spheroids were imaged immediately following the addition of the media for the 0 h time point, and imaged again 24 hours afterwards.

Imaging and data analysis

All images were acquired using a laser scanning confocal microscope (Leica TCS SP8; Leica Microsystems, Wetzlar, Germany). For 2D monolayer experiments, the bright-field image was used as a mask to measure the mean fluorescence intensity in individual cells using the freeware ImageJ. 3D invasion assay data were also analysed in ImageJ. In the 3D spheroid images, biosensor mean intensity over area was measured in the invading branches exclusively. The invading branches were selected manually at the *z*-plane of the image where the branches are in focus. For branches that are composed of multiple cells in different focal planes, the mean intensity was measured in each cell, when in focus. The intensity of the entire branch was then calculated as the average of the intensities of the cells composing the branch.

Statistical analysis

Data obtained from ImageJ were analysed using the statistical software GraphPad Prism 9. Free solution experiments were performed at least 3 times in different days with 3 replicates each day. Similarly, all other assays were performed at least 3 times in separate days. In monolayer experiments, at least 100 cells per case were analysed. For 3D spheroid assays, at least 15 spheroid branches were analysed in each case. All datasets were considered to follow a non-normal distribution. Therefore, non-parametric tests were utilized to compare across groups where possible. The tests used were: a Two-Way ANOVA test with a *post-hoc* Tukey test including multiple comparisons, a Brown–Forsythe and Welch ANOVA test and the Dunnet's T3 multiple comparisons test, and a two-tailed Mann–Whitney test. The following values were assigned to test

for significance: ns p-value >0.05, * p-value <0.05, ** p-value <0.01, *** p-value <0.001, and **** p-value <0.0001.

Results

Evaluating the quenching ability of the quencher sequences

Six quencher designs with varying amount and position of LNA monomers (4-LNA, 3-LNA, 2S-LNA, 2A-LNA, 1-LNA, and DNA) were designed and synthesized (Fig. 1B and ESI Table 1†). Since the binding affinity is critical for determining the specificity and the signal-to-noise ratio (SNR) of the biosensor, we first studied the binding affinity between the LNA probe and the quencher sequence (Fig. 2A and C). We evaluated the ability of the six different quencher sequences (Q) in reducing the signal of the free fluorophore probe (P). Data are shown as the normalized intensity *vs.* the Q : P ratio. With a high Q : P ratio, there was no significant difference across the LNA quenchers. At a lower Q : P ratio (*e.g.*, 1 : 1), the DNA quencher for the β-actin probe resulted in a significantly higher background noise (Fig. 2B). This observation shows the importance of incorporating LNA monomers for enhancing the quencher-probe binding. Furthermore, the biosensor signal was completely quenched if the Q : P ratio was over 2. Similar trends were also observed for the random probe (Fig. 2C and D).

Determining the influence of the quencher design on target detection

We next evaluated the effect of the quencher design on the sensing performance as the target has to displace the quencher for the fluorophore probe to fluoresce. The fluorophore probe and the quencher sequence concentrations were fixed at 250 nM and 750 nM respectively (*i.e.*, Q : P ratio of 3 : 1). The target (T) concentration was adjusted systematically from 0.1 to 1000 target-to-probe (T : P) ratio. The data were normalized to the intensity of the free fluorophore probe with no quencher in solution (Fig. 3A and C). The signal generally increased with the target concentration and the T : P ratio, supporting the dsLNA biosensor for detecting nucleic acid sequences. All quencher sequences (except 4-LNA) displayed an intensity similar to the free fluorophore probe at a T : P ratio of 10 : 1 (Fig. 3B and D). The 4-LNA quencher (*i.e.*, 4-LNA) had a significantly lower intensity and reached less than ~60% of the maximum intensity, even at high target concentrations. This observation suggests that a quencher sequence with a large amount of LNA monomers can limit the maximum signal of the dsLNA biosensor.

Our results show that the quencher sequence can influence both the background noise and the signal level. We, therefore, estimated the SNR of the dsLNA biosensor to evaluate the overall effect (Fig. 4 and ESI Table 2†). We calculated the SNR of each quencher by the formula denoted in the methods section and plotted it against increasing target concentrations (Fig. 4A and C). The design with the highest amount of LNA monomers displayed the lowest SNR across all target concentrations, which is explained by the reduced signal level. The difference in SNR was particularly apparent at a 10 : 1 T : P ratio (Fig. 4B and D). The DNA quencher (*e.g.*, no LNA modification) also showed a reduced SNR, primarily due to the higher background signal of the probe. At high/medium target concentrations, there is no significant difference in SNR between the 4-LNA and the DNA quenchers. In contrast, quencher sequences with 1 to 3 LNA monomers resulted in the highest SNR. Among the 3-LNA, 2S-LNA, 2A-LNA, and 1-LNA, there was no significant difference in SNR (Fig. 4B and D). These results suggest that the dsLNA sensor performance can be enhanced by an optimal number of LNA monomers.

Evaluating the specificity of the biosensors

In addition to the disassociation of the quencher sequence, additional noise in the dsLNA biosensor scheme can arise due to binding of the fluorophore probe to non-specific targets. A crucial aspect of the dsLNA biosensors' performance is the ability of the quencher sequence to competitively prevent non-specific binding. Therefore, we evaluated how the various quencher sequences affect the specificity of the dsLNA biosensor targeting β-actin against a non-specific random sequence (Fig. 5A). Similar to the target calibration, the data were normalized to the intensity of the free probe in solution. All quencher sequence designs demonstrated good selectivity against the non-specific random sequence, showing only minimal fluorescence intensity. Indeed, the intensity values were similar to the background intensity with a 3 : 1 Q : P ratio (Fig. 5B). Similar results were also observed for the random probe against the β-actin sequence (Fig. 5C and D). Furthermore, the 4-LNA quencher probe for β-actin biosensor was able to distinguish a single base mismatch target, suggesting its high specificity against similar targets (ESI Fig. S1†).

Testing the dsLNA biosensors in live and fixed cells

Next, we evaluated the performance and effect of the various quencher designs in live and fixed cells. In particular, the human cervical cancer cell line, HeLa, was used. In order to test the response of each quencher in live cells, we transfected HeLa cells with the 6 different quencher-probe configurations and measured the fluorescence intensity levels in the cells. The dsLNA probes targeting β-actin mRNA were transfected into the cells at a 3 : 1 Q : P ratio and left unperturbed for 24 hours to ensure uniform probe internalization. Fig. 6A and C shows representative images for the various biosensor configurations. The right panel shows a box plot of the mean intensity of cells within the monolayer for the various cases (Fig. 6B and D). For the β-actin probe, in agreement with the data in free solution, the signal intensity generally reduced with the number of LNA monomers, and the 4-LNA quencher sequence displayed the lowest signal. This is presumably due to the strong probe-quencher binding affinity of the 4-LNA quencher. In contrast, the highest signal level was obtained from the dsLNA biosensor with the DNA quencher. This is in good agreement with the biosensor calibration, where the DNA

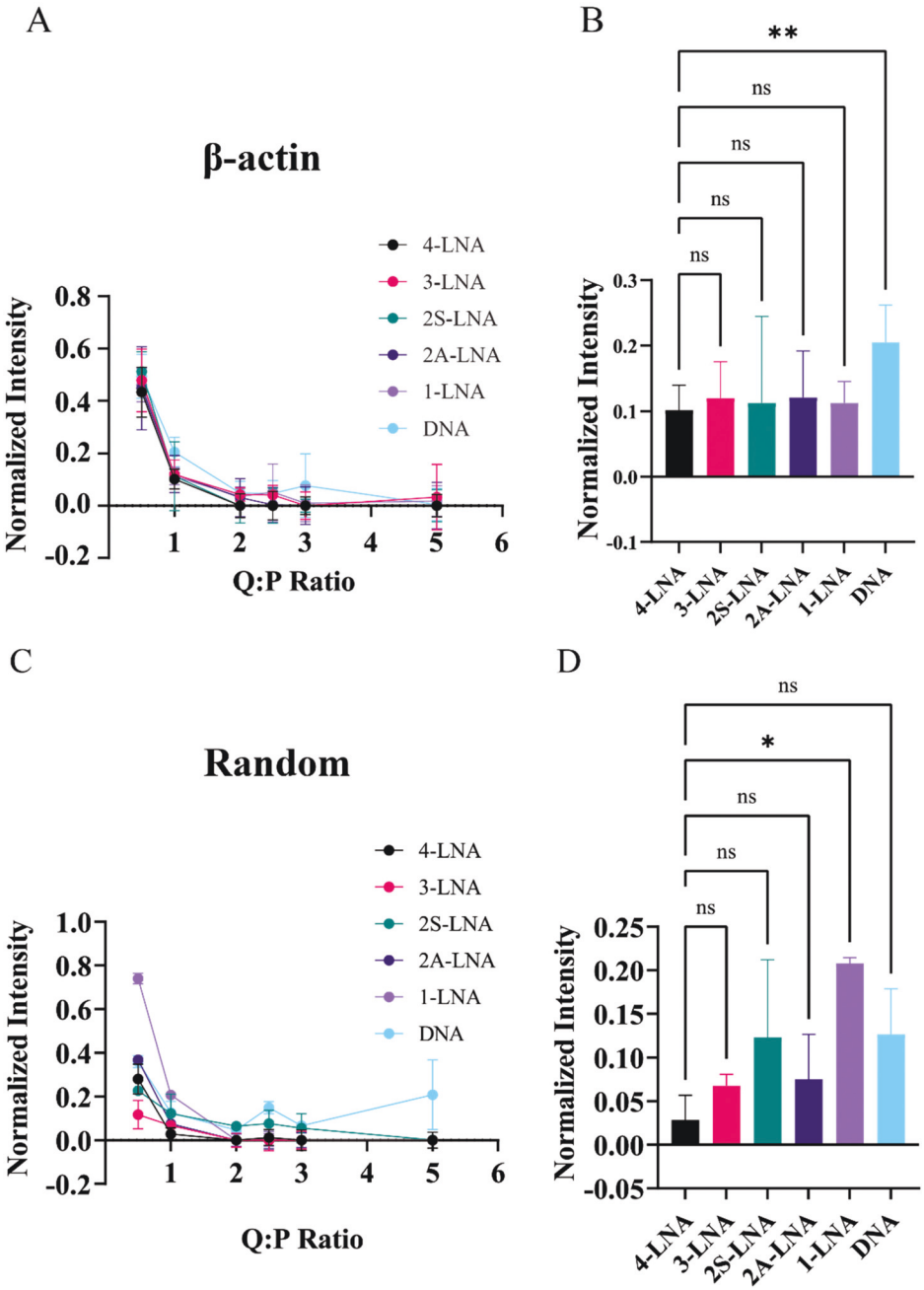

Fig. 2 Optimizing the quencher-to-probe (Q : P) ratio for various quencher designs. (A and C) Experimental characterization of the Q : P ratio for probes targeting β-actin mRNA and a random sequence. The probe concentration was 250 nM. The data are shown as a function of the Q : P ratio. The intensity is normalized by the intensity of the free probe. (B and D) Normalized intensity of the biosensor with a 1 : 1 Q : P ratio. Error bars represent the standard deviation. A two-way ANOVA test was used to evaluate differences among quenchers and Q : P ratios. A Brown–Forsythe and Welch ANOVA test and the Dunnet's T3 multiple comparisons test were used to evaluate differences among quenchers. Experiments were performed in triplicate on separate days. ns p-value >0.05, * p-value <0.05, and ** p-value <0.01.

quencher reached close to 100% the free probe signal. In contrast, the random probe did not have a strong dependence on the quencher design and did not show a clear trend (Fig. 6D). The weak relation suggests other factors (*e.g.*, autofluorescence and probe degradation) may also contribute to the background signal in live cells.

The experiment was also performed in fixed cells (Fig. 7). The DNA quencher showed a high signal with the β-actin probe and high noise with the random probe. In contrast, the 4-LNA quencher showed a low signal as well as the lowest noise levels. The signal level of the β-actin and random probe generally decreased with increasing amounts of LNA monomer

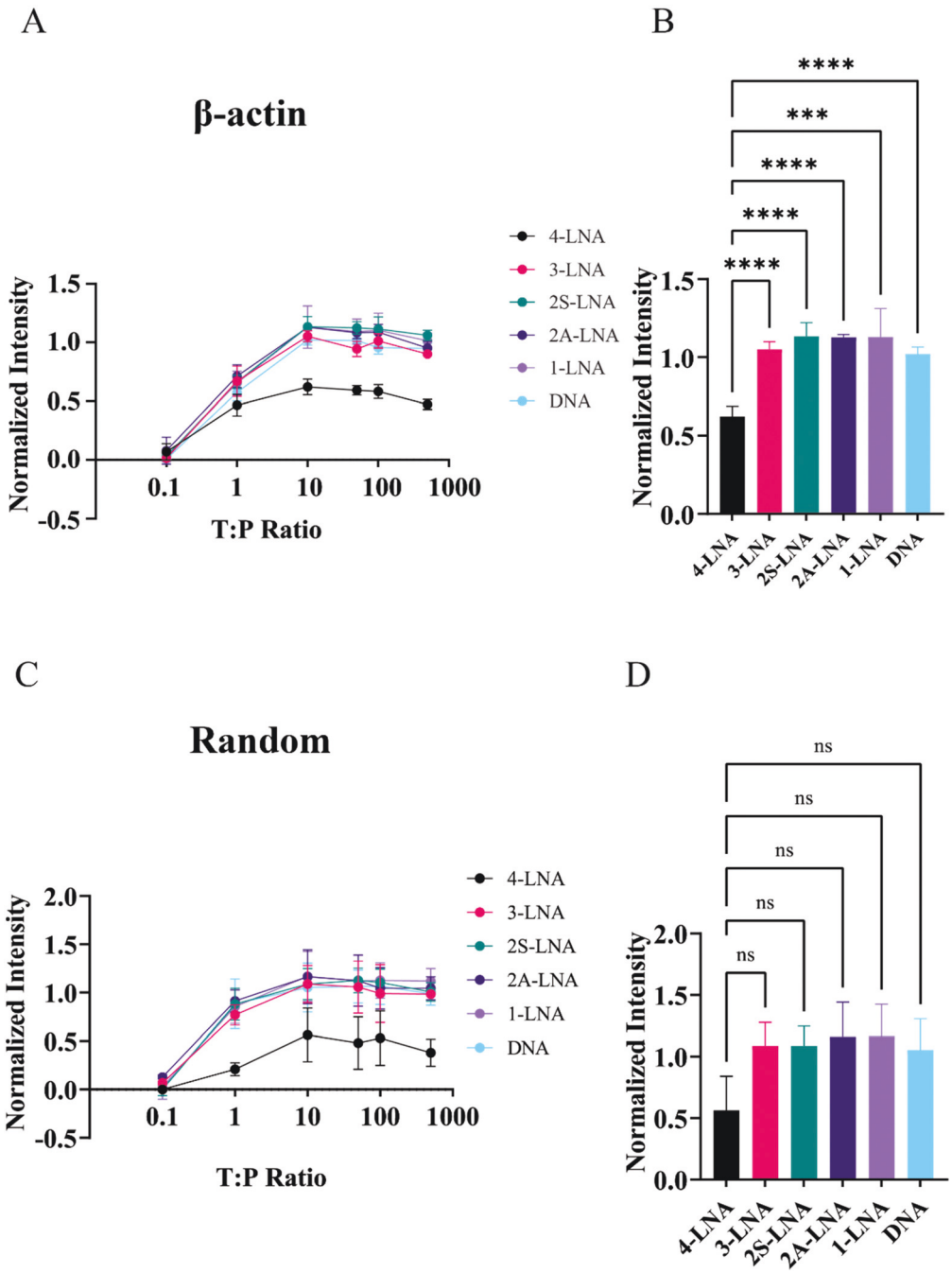

Fig. 3 Characterizing the target response for various quencher designs. (A and C) Experimental characterization of the sensing performance for probes targeting β-actin mRNA and a random sequence. The probe concentration was 250 nM, and the Q : P ratio was 3 : 1. The data are shown as a function of target-to-probe (T : P) ratio. The intensity is normalized by the intensity of the free probe. (B and D) Normalized intensity of the biosensor at a 10 : 1 T : P ratio. Error bars represent the standard deviation. A two-way ANOVA test was used to evaluate differences among quenchers and T : P ratios. A Brown–Forsythe and Welch ANOVA test and the Dunnet's T3 multiple comparisons test were used to evaluate differences among quenchers for a specific ratio. Experiments were performed in triplicate on separate days. ns p-value >0.05, *** p-value <0.001, and **** p-value <0.0001.

in the quencher sequence. The results were in good agreement with the free solution experiment.

Furthermore, we analysed the specificity of the dsLNA biosensor with a DNA quencher targeting β-actin mRNA and a random sequence in live cells (ESI Fig. S2†). The results showed that the β-actin probe had significantly higher fluorescence intensity compared to the random probe. Overall, our data supports the use of the dsLNA biosensor for single cell sensing in both live and fixed cells.

An important benefit of the dsLNA biosensor is the potential to be utilized in 3D culture models where other gene expression analysis techniques (*e.g.*, FISH) are more challen-

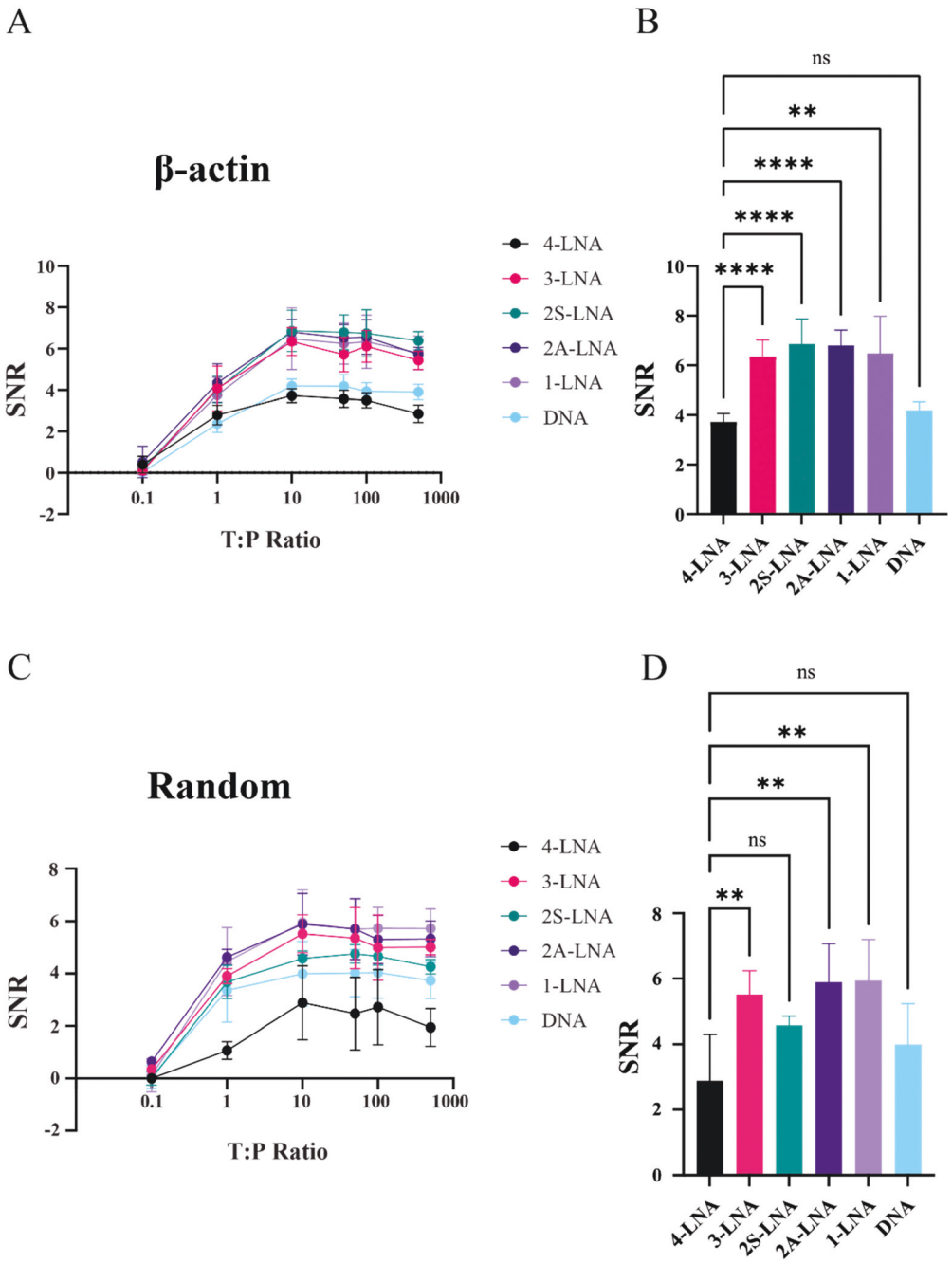

Fig. 4 Characterizing the signal-to-noise ratio (SNR) of various quencher designs. (A and C) Estimating the SNR for probes targeting β-actin mRNA and a random sequence. The probe concentration was 250 nM, and the Q : P ratio was 3 : 1. The data are shown as a function of target-to-probe (T : P) ratio. The SNR was determined by normalizing the intensity without target. (B and D) SNR of the biosensor with a 10 : 1 T : P ratio. Error bars represent the standard deviation. A two-way ANOVA test was used to evaluate differences among quenchers and T : P ratios. A Brown–Forsythe and Welch ANOVA test and the Dunnett's T3 multiple comparisons test were used to evaluate differences among quenchers for a specific ratio. ns p-value >0.05, p-value <0.01, and **** p-value <0.0001.

ging. We, therefore, demonstrated the use of dsLNA biosensors in invading 3D HeLa spheroids (Fig. 8). In particular, the biosensors with the 4-LNA quencher sequence and the DNA quencher sequence were tested. The dsLNA probes were transfected during 2D monolayer culture before spheroid formation to allow uniform probe distribution. We opted for a 3D invasion assay to test the performance of the dsLNA biosensor in invading sprouts. In the 3D tumor spheroid invasion assay, the spheroids were embedded in a blend of collagen I and basement membrane extract. The cancer cells formed invading sprouts that collectively invaded into the extracellular matrix. The biosensor signal was evaluated 24 hours after (Fig. 8A). In particular, we analysed the

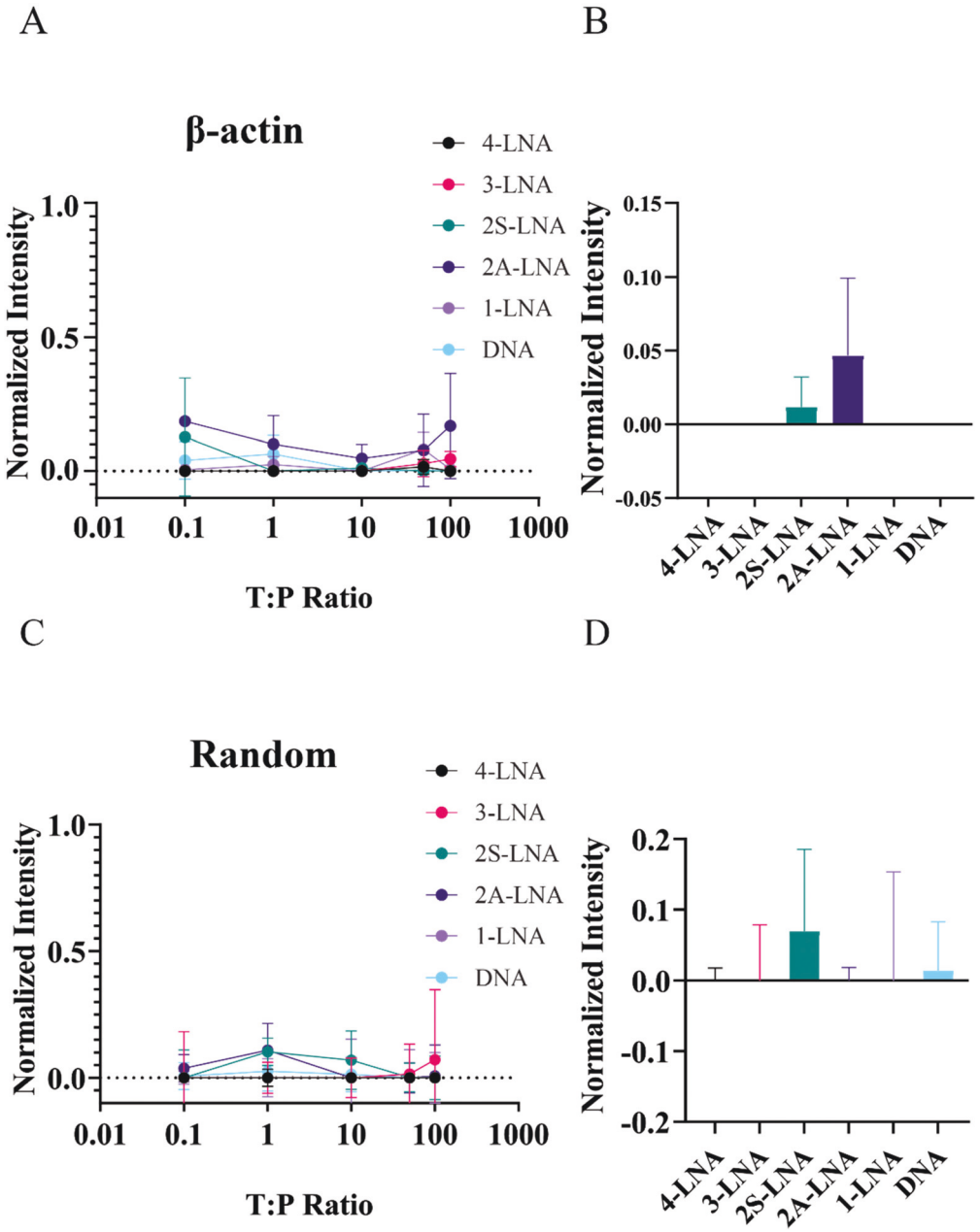

Fig. 5 Characterizing the specificity of the biosensors. (A and C) Normalized intensity against a non-specific target for the various quencher configurations. The probe concentration was 250 nM, and the Q : P ratio was 3 : 1. The data are shown as a function of target-to-probe (T : P) ratio. The intensity is normalized by the intensity of the free probe. (B and D) Normalized intensity for the different biosensor configurations with a 10 : 1 T : P ratio. Error bars represent the standard deviation. A two-way ANOVA test was used to evaluate differences among quenchers and T : P ratios. A Brown–Forsythe and Welch ANOVA test and the Dunnet's T3 multiple comparisons test were used to evaluate differences among quenchers for a specific ratio. Experiments were performed in triplicate on separate days.

invading branches protruding from the primary spheroids in order to compare between the DNA and 4-LNA biosensors (Fig. 8B). The intensity of the β-actin probe was significantly higher for the biosensor with the DNA quencher compared to the 4-LNA quencher (Fig. 8C). This observation further supports the notion that a large amount of LNA monomers can reduce the sensor signal due to a high binding affinity between the fluorophore probe and the quencher sequence.

Discussion

Novel biosensing techniques with high spatiotemporal resolution can greatly benefit the study of complex biological processes.[2,3] In this study, we investigated and optimized the performance of the dsLNA nanobiosensor for nucleic acid analysis and gene expression measurements in mammalian cells.[26] Importantly, the dsLNA biosensor is easy to implement

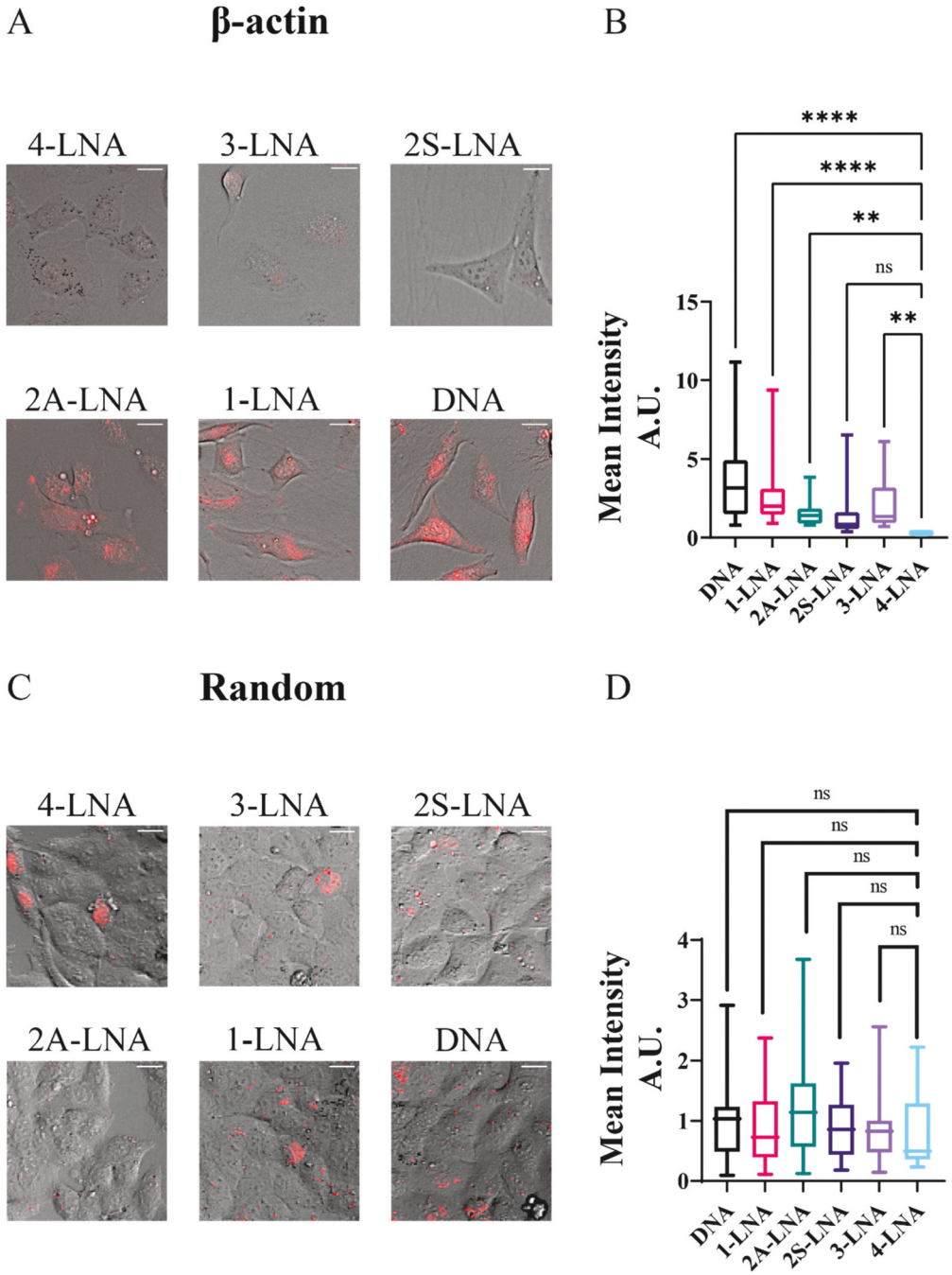

Fig. 6 Characterizing the biosensor performance of various quencher designs in live cells. (A and C) Representative fluorescence images of cancer cells (HeLa) transfected with probes targeting β-actin mRNA and a random sequence. Scale bars, 20 μm. (B and D) Box plots measuring mean intensity for each case normalized to the 4 LNA quencher signal and comparing it against the 4-LNA quencher design. The nonparametric Kruskal–Wallis test along with the Dunn's multiple comparisons test were used to compare across groups. ns p-value >0.05, ** p-value <0.01, and **** p-value <0.0001 (n = 34, 23, 15, 13, 12, 16 for DNA, 1-LNA, 2A-LNA, 2S-LNA, 3-LNA, 4-LNA respectively for the β-actin probe, n = 20 for all random quenchers).

and has a transfection efficiency for live cells (ESI Fig. S3†). Compared to biosensors based on conformational changes (*e.g.*, molecular beacons and DNA transformers),[8,9] the sensing performance of the dsLNA biosensor can be enhanced by adjusting the Q : P ratio. In comparison with other displacement sensors based on nanoengineered materials (*e.g.*, gold nanorods and graphene-based biosensors),[10,11] the ability to adjust the quencher sequence allows for easy optimization of the specificity and SNR. Additionally, it has been demonstrated that the double-stranded biosensing scheme can be

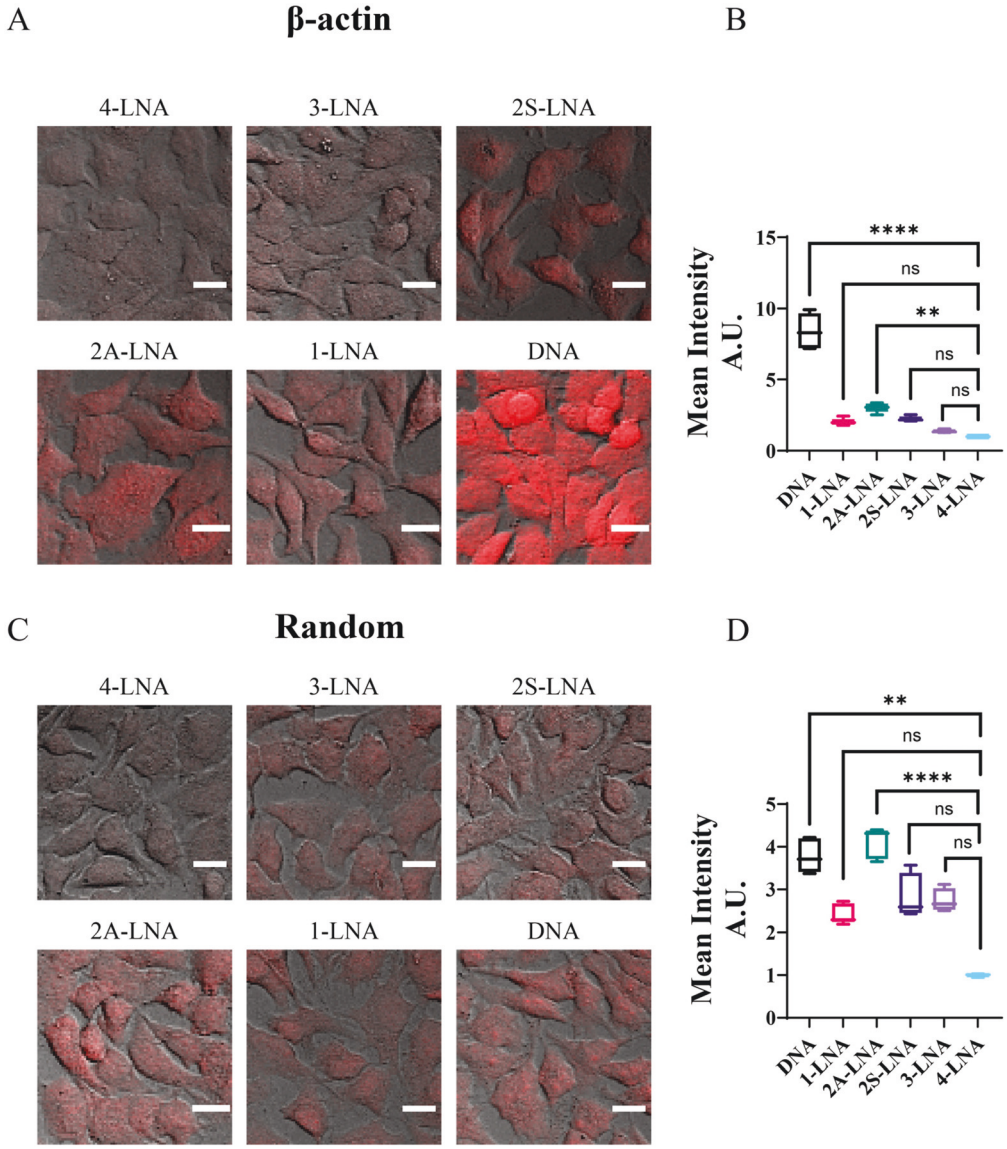

Fig. 7 Characterizing the biosensor performance of various quencher designs in fixed cells. (A and C) Representative fluorescence images of cancer cells (HeLa) hybridized with probes targeting β-actin mRNA and a random sequence. Scale bars, 20 μm. The cells were fixed and incubated with the biosensors without washing. (B and D) Box plots measuring mean intensity for each case normalized to the 4 LNA quencher signal and comparing it against the 4-LNA quencher design. The nonparametric Kruskal–Wallis test along with the Dunn's multiple comparisons test were used to compare across groups. ns p-value >0.05, ** p-value <0.01, and **** p-value <0.0001 (n = 5 fields with >800 cells per field).

easily implemented and applied in various biomedical applications, such as detecting single base mismatch[19] and quantifying mRNA and microRNA in live cells.[12–17]

The inclusion of LNA monomers in molecular probes has shown to improve the stability, signal-to-noise ratio, binding affinity, and resistance to degradation.[23,24] However, studies investigating the optimal placement and proportion of LNA monomers to optimize various biosensing applications are scarce. As demonstrated in this study, incorporating a large amount of LNA monomers does not necessary produce the best biosensing performance. If the binding affinity of the quencher sequence and fluorophore probe is too strong, it can also prevent target detection even at high concentrations of target, which is contributed by the strong LNA-LNA hybridization (*e.g.*, 4-LNA reached only ~50% of the maximum intensity).[24] In free solution, an optimal SNR was obtained with a small amount of LNA monomers (*e.g.*, 1–3) in the quencher sequence. The SNR was not significantly different in this range of LNA monomers. Furthermore, modifying the order of LNA monomers, as in the 2-LNA – A and 2-LNA – S quenchers, did not result in any significant differences in any of the assays performed. More experimentation regarding the placement of LNA monomers at equal proportions will be necessary to determine the importance of position in different biosensing scen-

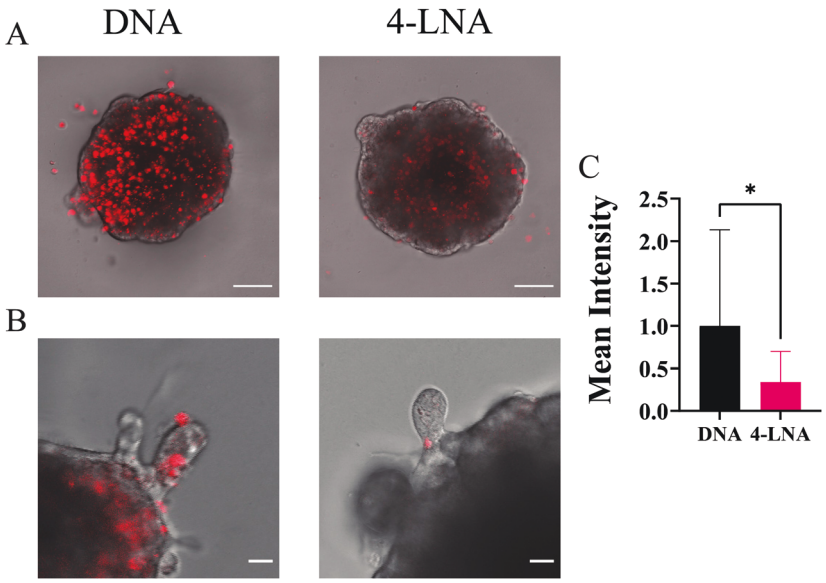

Fig. 8 Evaluating the biosensor performance in 3D spheroids. (A) Representative composite images of 3D spheroids. The cells (HeLa) were transfected with dsLNA targeting β-actin mRNA with DNA and 4-LNA quenchers. Scale bars, 100 μm. (B) Representative zoomed-in views of invading branches. Images were obtained 24 hours after loading of the invasion matrix. Scale bars, 20 μm. (C) Mean intensity of the invading branches after 24 hours for each case. The nonparametric Mann–Whitney test was used to compare across cases.

arios. In this study, the number of LNA monomers resulted in the strongest factor in determining the characteristics of a quencher design for various applications.

Notably, there is a trade-off between the sensor signal and the noise level. The dsLNA detects only a portion of the target sequence based on equilibrium binding.[18,19] This is an important consideration for live cell imaging as additional, uncontrollable sources can contribute to the overall background noise. If binding to a larger portion of the target sequence is desired (*e.g.*, due to autofluorescence in the environment or low abundance targets), a quencher sequence with low-to-no LNA monomers (*e.g.*, DNA quencher) can be applied. If non-specific binding of similar targets is an issue, the amount of LNA monomers (and potentially the length of the quencher sequence) can be increased to improve the quencher-probe binding affinity. In general, we recommend that researchers use low-to-no LNA monomers (*e.g.*, DNA quencher) in live and fixed cell imaging. In free solution assays we recommend using 1-LNA–3-LNA monomers for an optimal signal to noise ratio and reliable performance. However, if high specificity is required, a large number of LNA monomers (*e.g.*, 4-LNA quencher) should be applied.

Conclusions

This study optimizes the dsLNA biosensors for nucleic acid analysis. The results reveal trade-offs between sensitivity and specificity when incorporating LNA monomers in the quencher design. Therefore, we recommend that researchers should take into account these considerations to improve the performance of dsLNA biosensors in biochemical assays and live cell imaging accordingly.

Conflicts of interest

There are no conflicts to declare.

Acknowledgements

This work was supported by National Science Foundation Biophotonics program (1802947) and RECODE program (2033673).

Notes and references

1 Y. Du and S. Dong, *Anal. Chem.*, 2017, **89**, 189–215.
2 S. A. Vilchez Mercedes, F. Bocci, H. Levine, J. N. Onuchic, M. K. Jolly and P. K. Wong, *Nat. Rev. Cancer*, 2021, **21**, 592–604.
3 J. Sun, Y. Xiao, S. Wang, M. J. Slepian and P. K. Wong, *J. Lab. Autom.*, 2015, **20**, 127–137.
4 P. Torab, Y. Yan, M. Ahmed, H. Yamashita, J. I. Warrick, J. D. Raman, D. J. DeGraff and P. K. Wong, *Cells*, 2021, **10**, 3084.
5 A. M. Femino, F. S. Fay, K. Fogarty and R. H. Singer, *Science*, 1998, **280**, 585–590.
6 J. M. Levsky, S. M. Shenoy, R. C. Pezo and R. H. Singer, *Science*, 2002, **297**, 836–840.

7 G. Bao, W. J. Rhee and A. Tsourkas, *Annu. Rev. Biomed. Eng.*, 2009, **11**, 25–47.
8 K. Wang, Z. Tang, C. J. Yang, Y. Kim, X. Fang, W. Li, Y. Wu, C. D. Medley, Z. Cao, J. Li, P. Colon, H. Lin and W. Tan, *Angew. Chem., Int. Ed.*, 2009, **48**, 856–870.
9 Y. Wan, N. Zhu, Y. Lu and P. K. Wong, *Anal. Chem.*, 2019, **91**, 2626–2633.
10 S. Wang, R. Riahi, N. Li, D. D. Zhang and P. K. Wong, *Adv. Mater.*, 2015, **27**, 6034–6038.
11 H. Zhang, H. Zhang, A. Aldalbahi, X. Zuo, C. Fan and X. Mi, *Biosens. Bioelectron.*, 2017, **89**, 96–106.
12 J. Gao, H. Li, P. Torab, K. E. Mach, D. W. Craft, N. J. Thomas, C. M. Puleo, J. C. Liao, T. H. Wang and P. K. Wong, *Nanomedicine*, 2019, **17**, 246–253.
13 Z. S. Dean, P. Elias, N. Jamilpour, U. Utzinger and P. K. Wong, *Anal. Chem.*, 2016, **88**, 8902–8907.
14 R. Riahi, J. Sun, S. Wang, M. Long, D. D. Zhang and P. K. Wong, *Nat. Commun.*, 2015, **6**, 6556.
15 R. Riahi, Z. Dean, T. H. Wu, M. A. Teitell, P. Y. Chiou, D. D. Zhang and P. K. Wong, *Analyst*, 2013, **138**, 4777–4785.
16 Z. S. Dean, R. Riahi and P. K. Wong, *Biomaterials*, 2015, **37**, 156–163.
17 N. E. Larkey, C. K. Almlie, V. Tran, M. Egan and S. M. Burrows, *Anal. Chem.*, 2014, **86**, 1853–1863.
18 V. Gidwani, R. Riahi, D. D. Zhang and P. K. Wong, *Analyst*, 2009, **134**, 1675–1681.
19 D. Meserve, Z. Wang, D. D. Zhang and P. K. Wong, *Analyst*, 2008, **133**, 1013–1019.
20 C. Y. J. Yang, C. D. Medley and W. H. Tan, *Curr. Pharm. Biotechnol.*, 2005, **6**, 445–452.
21 W. Zhang, *Adv. Exp. Med. Biol.*, 2014, **811**, 19–43.
22 C. J. Yang, L. Wang, Y. Wu, Y. Kim, C. D. Medley, H. Lin and W. Tan, *Nucleic Acids Res.*, 2007, **35**, 4030–4041.
23 M. Petersen, K. Bondensgaard, J. Wengel and J. P. Jacobsen, *J. Am. Chem. Soc.*, 2002, **124**, 5974–5982.
24 B. Vester and J. Wengel, *Biochemistry*, 2004, **43**, 13233–13241.
25 L. Wang, C. J. Yang, C. D. Medley, S. A. Benner and W. Tan, *J. Am. Chem. Soc.*, 2005, **127**, 15664–15665.
26 S. Huang, J. Salituro, N. Tang, K. C. Luk, J. Hackett, P. Swanson, G. Cloherty, W. B. Mak, J. Robinson and K. Abravaya, *Nucleic Acids Res.*, 2007, **35**, e101.